Identification of key biomarkers associated with immune modulation in triple-negative breast cancer

Soong June Bae

The Graduate School
Yonsei University
Department of Medicine

Identification of key biomarkers associated with immune modulation in triple-negative breast cancer

A Dissertation Submitted
to the Department of Medicine
and the Graduate School of Yonsei University
in partial fulfillment of the
requirements for the degree of
Doctor of Philosophy in Medical Science

Soong June Bae

December 2024

This certifies that the Dissertation of Soong June Bae is approved

Thesis Supervisor Joon Jeong

Thesis Committee Member Yoon Jin Cha

Thesis Committee Member Airi Han

Thesis Committee Member Seho Park

Thesis Committee Member Jee Hung Kim

The Graduate School
Yonsei University
December 2024

ACKNOWLEDGEMENTS

First and foremost, I wish to place on record my heartfelt and sincere gratitude to my advisor, Prof. Joon Jeong, for the continuous support of my Ph.D. study and related research, as well as for his patience, motivation, and immense knowledge. His guidance has been invaluable in helping me complete this thesis throughout my research. His scientific attitude and profound knowledge have guided me in the right direction. It has been a wonderful journey in cancer research with him, one that I hope will continue.

I extend my sincere gratitude to Prof. Yoon Jin Cha and Jee Hung Kim, who provided access to breast cancer samples and supported various analyses. Without their invaluable support and leadership, this research would not have been possible.

I would like to thank Prof. Airi Han for her insightful comments and encouragement, which inspired me to broaden my research from various perspectives.

I am deeply indebted to Prof. Seho Park, who has been a tremendous mentor to me. I am grateful for his encouragement of my research and the valuable time he has generously provided.

Lastly, I would like to thank my family—my wife (Ji Yeon Kim) and son (Joon Hoo Bae)—who have been my endless source of purpose throughout this journey and beyond.

TABLE OF CONTENTS

LIST OF FIGURES

LIST OF TABLES

ABSTRACT

Identification of key biomarkers associated with immune modulation in triple-negative breast cancer

Triple-negative breast cancer (TNBC) is a highly heterogeneous and aggressive subtype of breast cancer, with the features of tumor microenvironment and the underlying molecular mechanisms of immune-regulation remaining largely elusive. This study aimed to explore the immune landscape of TNBC by assessing tumor-infiltrating lymphocytes (TILs) level, programmed cell death ligand 1 (PD-L1) expression, and the degree of TIL infiltration within the tumor. Utilizing the GeoMX Digital Spatial Profiler platform, we also performed spatially resolved transcriptomic profiling of tumor, immune, and stromal cells, focusing on the distinctions between immune-activated and immune-suppressed phenotypes. Immune-activated phenotypes, characterized by high TILs, PD-L1 positivity, and close proximity between tumor cells and TILs, were found to correlate with the basal-like immune-activated subtype based on transcriptomic alterations derived solely from tumor cells. These phenotypes were also associated with the upregulation of known immune-related pathways. In contrast, immune-suppressed phenotypes were linked to pathways involved in tumor progression, such as epithelial-mesenchymal transition, TGF-beta signaling, and angiogenesis. Notably, our transcriptomic analysis suggests that tumor cells play a more dominant role than immune cells in shaping the immune phenotype, as indicated by the greater number of differentially expressed genes in tumor cells rather than immune cells. Stratifying patients based on TILs and PD-L1 status revealed that the TIL+PD-L1+ subtype exhibited the most favorable prognosis, a finding further supported by TIL+PD-L1+ signature with excellent survival outcomes in public gene datasets. Conversely, the TIL-PD-L1- subtype displayed characteristics of an "cold" tumor, potentially driven by desmoplastic changes within the tumor microenvironment. Interestingly, the TIL+PD-L1- subtype, despite a high TILs level, was associated with poorer prognosis, likely due to a higher proportion of myeloid cells, decreased activity of immune cells, and increased activation of the adipogenesis pathway across cell types. This finding underscores that in the TIL+PD-L1- subtype, immune cell activity remains low even when TILs infiltrate the intra-tumoral region, highlighting PD-L1 as a critical marker reflecting

the immune system status in patients with high TILs. In summary, this study emphasizes the clinical significance of integrating TILs and PD-L1 expression as prognostic biomarkers in TNBC and underscores the central role of tumor cells in dictating immune phenotypes. Furthermore, our findings suggest potential underlying mechanisms and target genes regarding the immune system regulation in TNBC. Based on these insights, future research is warranted to develop targeted therapies, especially for immune-suppressed subtypes, aiming to improve clinical outcomes for patients with TNBC.

Key words : triple-negative breast cancer, tumor-infiltrating lymphocytes, programmed cell death ligand 1, tumor-immune microenvironment, digital spatial transcriptomics.

I. INTRODUCTION

Triple-negative breast cancer (TNBC), defined by the absence of hormone receptors (estrogen receptor [ER]-negative and progesterone receptor [PR]-negative) and human epidermal growth factor receptor 2 (HER2), accounts for approximately 10-20% of all breast cancers[1,2]. TNBC is the most aggressive subtype among breast cancer subtypes, with a poor prognosis due to the lack of well-defined therapeutic targets[3]. Recently, TNBC has been identified as a more immunogenic tumor compared to other breast cancer subtypes. Moreover, immune-related biomarkers, most notably tumor-infiltrating lymphocytes (TILs), have been shown to be strongly associated with treatment response and prognosis in TNBC[4-6].

Recent advancements in immunobiology have facilitated the incorporation of immunotherapies, such as Programmed Cell Death Protein-1 (PD-1) and Programmed Cell Death Ligand-1 (PD-L1) inhibitors, into the treatment of TNBC[7,8]. Notably, the addition of pembrolizumab, a PD-1 inhibitor, to palliative chemotherapy as first-line treatment for metastatic TNBC significantly improved clinical outcomes, particularly in patients expressing PD-L1[9,10]. Furthermore, the combination of pembrolizumab with neoadjuvant chemotherapy markedly increased the pathologic complete response (pCR) as well as survival rates in patients with Stage II or III TNBC[11-13]. Based on these findings, pembrolizumab has become an FDA-approved treatment regimen for both early-stage and metastatic TNBC.

Nevertheless, the molecular biology behind the variability in the immune-related tumor microenvironment within TNBC remain unclear. While chemotherapy combined with pembrolizumab has improved clinical outcomes for patients with TNBC, considering the associated adverse events and financial toxicity[14], there is a need for biomarkers to guide personalized treatment[15]. Although numerous analyses with RNA-sequencing data have been conducted to address this, most previous studies have employed bulk-sequencing without distinguishing between different cell types within the tumor microenvironment, which is a notable limitation[16,17].

In this study, we analyzed the clinical characteristics associated with immune system status in triple-negative breast cancer (TNBC), focusing on TILs level, PD-L1 expression, and the tumor-immune microenvironment (TIME) subtypes. Furthermore, we utilized the Nanostring GeoMX Digital Spatial Profiler (DSP) to enable spatially resolved characterization of tumor, immune, and stromal cells, aiming to decipher the features of the tumor microenvironment based on immune system status. Through this approach, we tried to identify potential underlying mechanisms and key biomarkers that regulate the immune system in TNBC.

II. MATERIALS AND METHODS

2.1. Study population

Between January 1999 and December 2014, we retrospectively identified 603 women diagnosed with triple-negative breast cancer who underwent upfront surgery followed by adjuvant therapy at Gangnam Severance Hospital, Yonsei University. From this cohort, tissue microarray (TMA) blocks were constructed from 198 patients with appropriate surgical specimens for further analysis, with TILs level being assessable in 159 cores. Among these, PD-L1 status evaluated using SP142 and 22C3 antibodies, and tumor-immune microenvironment (TIME) subtypes were successfully assessed in 104 patients. Additionally, GeoMX digital spatial transcriptomics was conducted on 96 samples (Figure. 1).

We collected comprehensive clinicopathological data, including age at diagnosis, tumor grade, estrogen receptor (ER) status, progesterone receptor (PR) status, human epidermal growth factor receptor 2 (HER2) status, Ki-67 index, TILs level, PD-L1 status, TIME subtypes, pathological T and N stages, adjuvant treatments such as chemotherapy and radiotherapy, and survival outcomes. Pathological T and N stages were determined according to the anatomical staging system outlined in the 8th edition of the American Joint Committee on Cancer (AJCC) guidelines. All pathological data were derived from surgical specimens.

The study protocol was reviewed and approved by the Institutional Review Board of Gangnam Severance Hospital, Yonsei University, Seoul, Korea. This study was conducted in accordance with the principles of the Declaration of Helsinki. Given the retrospective nature of the study, the requirement for written informed consent was waived by the Institutional Review Board.

2.2. TMA construction, TILs level, PD-L1, and TIME assessment

A representative tumor area was selected from hematoxylin and eosin (H&E)-stained slides, and the corresponding spot was marked on the surface of the paraffin-embedded block. The selected area was then extracted using a hollow needle to produce a 3-mm tissue core, which was subsequently embedded into a 10×5 recipient block. Each tissue core was assigned a unique TMA location number, which was linked to a comprehensive clinicopathological information.

Stromal TILs were evaluated in all cores containing invasive tumor cells, following the guidelines proposed by the International TIL Working Group[18]. Mononuclear cells, including lymphocytes and plasma cells, were quantified, excluding polymorphonuclear leukocytes, and the average TILs level was reported as a percentage[19]. For statistical purposes, a 30% cutoff value was used to categorize patients into low TIL (<30%) and high TIL (≥30%) groups[20,21].

Tissue microarray (TMA) sections, 3 μm in thickness, were obtained from formalin-fixed, paraffin-embedded blocks as previously described[22]. Following deparaffinization with xylene and rehydration in graded alcohol solutions, immunohistochemistry (IHC) was conducted using the Ventana Discovery XT Automated Slide Stainer (Ventana Medical System, Tucson, AZ, USA). Antigen retrieval was performed using Cell Conditioning 1 buffer (citrate buffer, pH 6.0; Ventana Medical Systems). Tissue sections were then incubated with primary antibodies specific to PD-L1 (prediluted, clone SP142, Ventana Medical Systems; 1:50, clone 22C3, DAKO). Appropriate positive and negative controls were included in each assay.

We classified each patient into four tumor immune microenvironment (TIME) subtypes based on the density and location of TILs in the tumor margin and tumor core (including both stromal and epithelial regions) on whole slide images[23]: i) Immune-Desert (ID): characterized by low TILs abundance in both the tumor margin and core; ii) Margin-Restricted (MR): TILs are predominantly confined to the tumor margin, with no presence in the tumor core; iii) Stroma-Restricted (SR): TILs are present in both the tumor margin and core but are restricted to the stromal region within the tumor core; iv) Fully-Inflamed (FI): TILs are abundant in both the tumor margin and core, with infiltration into both the stromal and intratumoral regions of the tumor core.

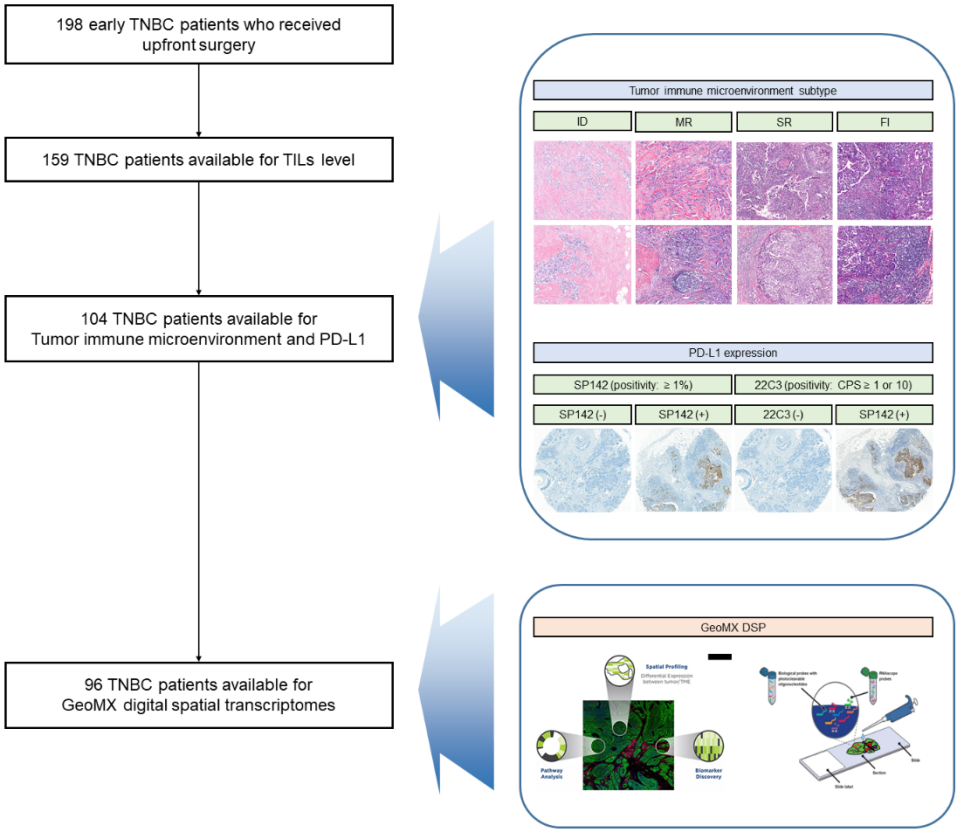

Figure 1. Study population.

2.3. GeoMX Digital Spatial Profiling Protocol

The protocol for the GeoMX DSP is outlined in Figure. 2A. This platform was employed to quantify antibody binding within user-defined regions of interest (ROIs) on 5-micron sections from a previously constructed tissue microarray TMA of a TNBC cohort. Following the manufacturer's protocol, four TMA slides, each consisting of 3 x 3 mm formalin-fixed, paraffin-embedded TNBC tumor cores derived from representative tumor blocks, were hybridized with the NanoString Technologies Whole Transcriptome Atlas barcoded probe set, targeting approximately 18,000 genes. Subsequently, the slides were stained with an antibody cocktail containing three fluorophore-labeled "morphological" antibodies and the nuclear dye SYTO-13 to guide ROI selection and masking. The antibodies used included anti-pan-cytokeratin (panCK, AlexaFluor 532) and anti-CD45 (AlexaFluor 594), alongside the nuclear stain SYTO-13, all of which were sourced from NanoString and applied to the slides at a 1:40 dilution. Each TMA slide was then scanned using the GeoMX digital analyzer,

resulting in a composite three-color/channel digital image based on the two fluorophore-tagged antibodies (panCK and CD45) and the SYTO-13 nuclear dye (Figure 2A).

All immunofluorescent images from the representative TMA cores were reviewed by an experienced breast pathologist (Dr. Cha). Per tissue core, one to three 600-micron circular ROIs were selected to capture a region enriched in viable tumor with adjacent stroma. ROI segmentation involved assignment of "masks" to encompass the "tumor cells" segment composed of the panCK-positive cells, the 'immune cells" segment composed of the CD45-positive cells, and the "stromal cells" segment composed of panCK-ngeative/CD45-negative/SYTO13-positive cells. Each ROI was inspected visually to ascertain that the computer-generated masks precisely encompassed the appropriate segments (Figure 2B). ROI selection/segmentation was blinded to TILs level, PD-L1 SP142 or 22C3 immunohistochemical assay status, and TIME subtypes; however, for assignment of immune-related status for this study, TILs level, PD-L1 immunohistochemical assay status, and TIME subtypes were visually confirmed by the same pathologist after the GeoMX DSP experiment was complete.

A total of 374 ROI segments were designated, comprising 136 "tumor cell" segments, 109 "immune cell" segments, and 129 "stromal cell" segments, including a total of 239,385 cells (107,766 tumor cells, 61,632 immune cells, and 69,987 stromal cells). The median number of cells per ROI segment was 490 (range: 66–2,348), and RNA sequencing was subsequently performed for each ROI segment (Figure 2C).

2.4. Transcriptomics analysis

Data processing was performed using the official piplelines provided by NanoString Technologies, which are available on the Bioconductor wevsite. We utilized the NanoStringNCTools, GeomxTools, and GeoMXWorkflows pachages in R to conduct data loading, quality control (QC) and pre-processing, normalization, unsupervised analysis, differential expression analysis, and visualization, Following this, we confrimed that RNA expression differences were more distinctly divided by cell segments rahter than by TILs, recurrence status, or TMA slides (Figure 2D).

Siginificant differentially expressed genes (DEGs) for each variable were defined as those with a flod change greater than 0.5 and a *P*-value below 0.05. In addition, gene setes with an adjusted P-value of 0.05 or lower were visualized. For pathway analysis, we used Gene Set Enrichment Analysis (GSEA) with the MsigDB Hallmark gene set. A gene signature for the TIL-PD-L1 based subtype was constructed using the 163 most significant DEGs in tumor segments. To estimate inferred cell fractions in our immune segments, we used the CIBERSORTx web tool. The signature matrix was generated using public single-cell RNA sequencing data, and based on this matrix, we imputed immune cell fractions within the immune segments.

(A)

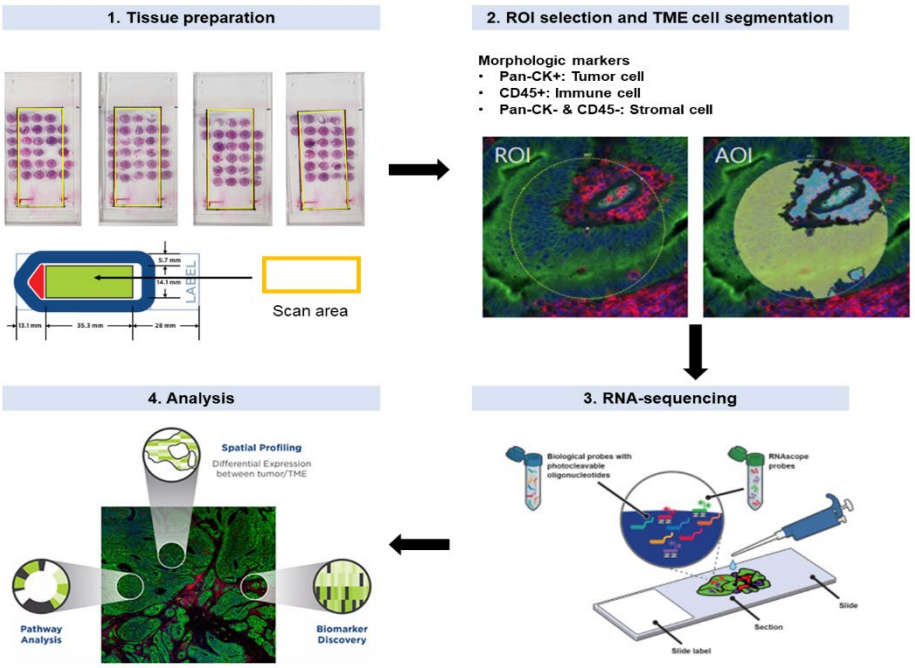

(B)

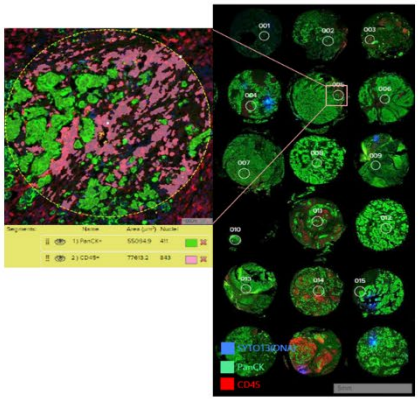

(D)

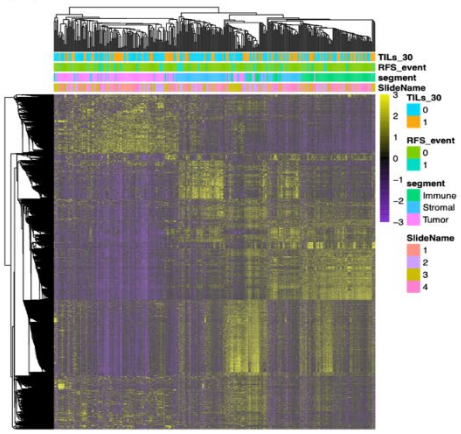

(C)

	Tumor	Immune	Stromal	Total
ROI segment	136	109	129	374
Total Cell number	107,766	61,632	69,987	239,385
Median (range)	690 (102-2,348)	420 (66-2,339)	437 (181-1,597)	490 (66-2,348)

Figure 2. GeoMX digital spatial transcriptomes. (A) Workflow of GeoMX digital spatial profiler. (B) Representative image of tissue microarray stained with morphological antibody and region-of-interest (ROI) with cell segmentation. (C) Number of ROI segments and cells across the cell types. (D) Gene expression between the cell segments.

2.5. Statistical analysis

We compared clinicopathologic characteristics and survival outcomes between the groups divided by immune phenotype. According to the Standardized Definitions for Efficacy End Points criteria[24], recurrence-free interval (RFI) was defined as the time from diagnosis to the first event of invasive local, regional, distant recurrence and death from breast cancer. Overall survival (OS) was defined as the time from diagnosis to the first death event for any reason.

Categorical variables were compared using the chi-squared test or Fisher's exact test. The Kaplan-Meier method was used to estimate the survival rate, and the results between the groups were compared using the log-rank test. The hazard ratio (HR) with its associated 95% confidence interval (CI) was estimated using the Cox regression model adjusted for key baseline prognostic factors (age: < 50 vs. ≥ 50, tumor grade: 1 or 2 vs 3, Ki-67 index: < 20% vs. ≥ 20%, pT stage: 1 vs. ≥ 2, pN status: negative vs. positive). All tests were two-sided, and *P*-values less than 0.05 were considered statistically significant. All statistical analyses were performed using SPSS version 27 software (SPSS, Armonk, NY, USA).

III. RESULTS

3.1. Clinical and transcriptomic features by TILs level

TILs level was successfully evaluated in 159 patients with early TNBC who received upfront surgery. The baseline characteristics of the patients are described in Table 1. Overall, age < 50 years was observed in 81 (50.9%) patients, and 114 (75.5 %) patients were tumor grade 3. The majority of patients had a high Ki-67 index (84.9%), pathological T1 or T2 stage (95.6%), and were node-negative (71.7%]). In addition, most patients (92.5%) received adjuvant chemotherapy after curative surgery. Of 159 patients, 72 (45.2%) belonged to the high TILs group, and 87 (54.8%) belonged to the low TILs group. The two groups had no difference in baseline characteristics (Table 1).

During a median follow-up of 121 months, the patients with high TILs exhibited a better prognosis than those with low TILs (Figure 3A-B). The 10-year RFI was 95.2% in the high TILs group, compared to 74.6% in the low TILs group (log-rank $P = 0.011$). Similarly, the 10-year and OS was 95.2% in the high TILs group versus 74.6% in the low TILs group (log-rank $P = 0.005$). Furthermore, high TILs level was an independent predictor of favorable clinical outcomes in terms of RFI (HR, 0.38; 95% CI, 0.15 to 0.98, $P = 0.045$) and OS (HR, 0.36; 95% CI, 0.15 to 0.91, $P = 0.031$) in multivariable analysis.

We identified DEGs by TILs level across various cell types, including tumor, stromal, and immune cells. Intriguingly, 92 genes were nominally differentially expressed in tumor cells between the high and low TILs groups, while 30 genes and 10 genes were differentially expressed in stromal and immune cells, respectively (Figure 3C). Pathway analyses of these DEGs showed that immune

system activation-related pathways, such as interferon (IFN)-alpha and -gamma responses, were upregulated in the high TILs group. In contrast, pathways associated with epithelial-mesenchymal transition (EMT) and TGF-beta signaling were downregulated across all cell types (Figure 3D). We also estimated the proportion of Burstein subtypes based on transcriptomic data derived exclusively from tumor cells[25]. Compared with the low TILs group, the high TILs group had a higher prevalence of basal-like immune-activated (BLIA) subtype (Figure 3E). Meanwhile, when deconvolution analysis was performed using CIBERSORTx on transcriptomic data derived exclusively from immune cells, the two groups had no difference in the proportions of T cells and B cells (Figure 3F).

Table 1. Baseline characteristics according to TILs level.

Variables	Low TIL (N = 87)	High TIL (N = 72)	Total (N=159)	*P*-value
Age				0.674
< 50	43 (49.4)	38 (52.8)	81 (50.9)	
≥ 50	44 (50.6)	34 (47.2)	78 (49.1)	
Tumor grade*				0.527
1 or 2	22 (26.5)	15 (22.1)	37 (24.5)	
3	61 (73.5)	77.9)	114 (75.5)	
Ki-67				0.085
< 20%	17 (19.5)	7 (9.7)	24 (15.1)	
≥ 20%	70 (80.5)	65 (90.3)	135 (84.9)	
pT stage				0.515
1	39 (44.8)	36 (50.0)	75 (47.2)	
≥ 2	48 (55.2)	36 (50.0)	84 (52.8)	
pN status				0.626
Negative	61 (70.1)	53 (73.6)	114 (71.7)	
Positive	26 (29.9)	19 (26.4)	45 (28.3)	
Chemotherapy				0.387
Yes	79 (90.8)	68 (94.4)	147 (92.5)	
No	8 (9.2)	4 (5.6)	12 (7.5)	
Radiotherapy				0.905
Yes	56 (64.4)	47 (65.3)	103 (64.8)	
No	31 (35.6)	25 (34.7)	56 (35.2)	

*Missing values.

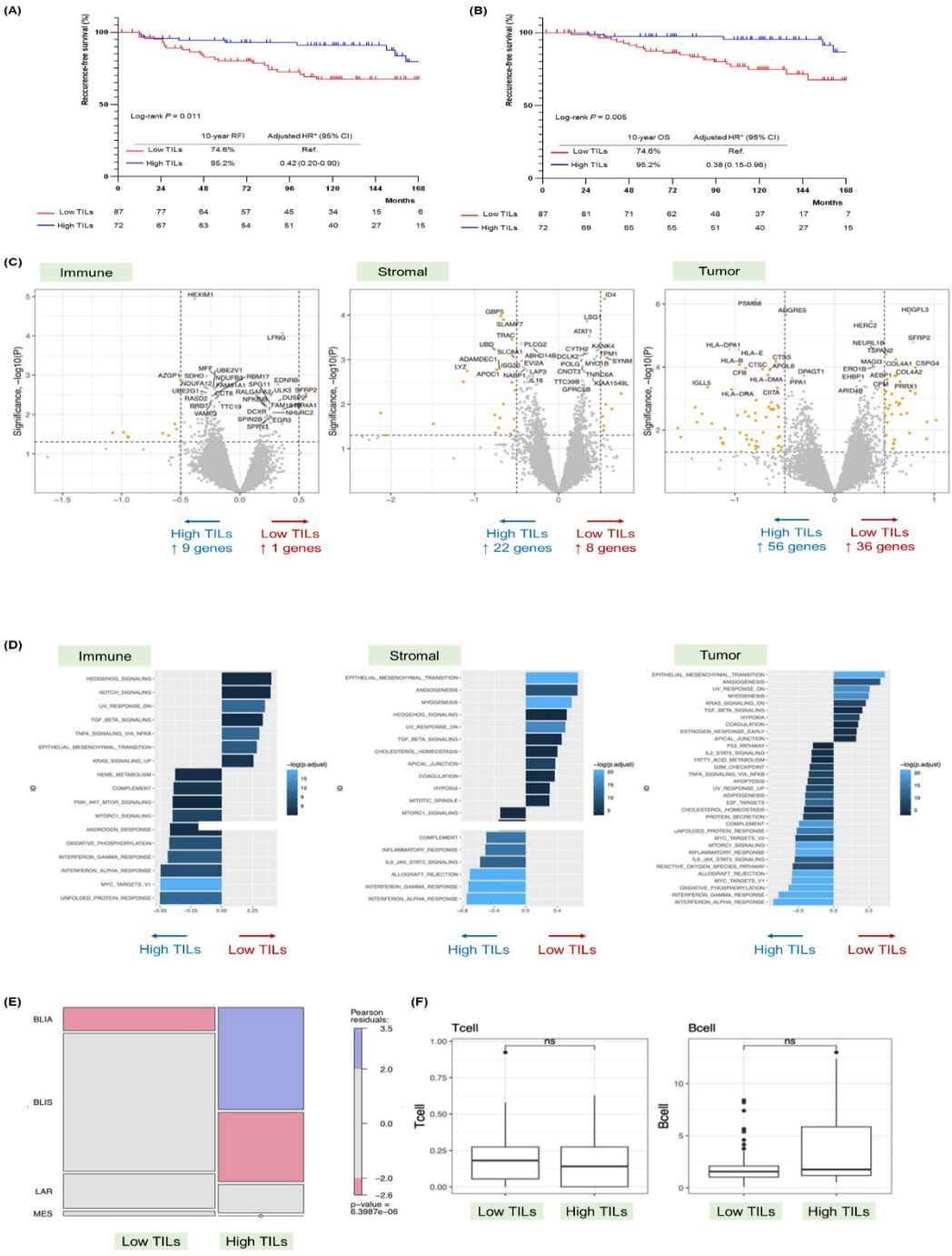

Figure 3. Clinical and transcriptomic features by TILs level. (A) Recurrence-free interval and (B) overall-survival according to TILs level. (C) Differentially expressed genes according to TILs level. (D) Pathway analyses according to TILs level. (E) Proportion of Burstein subtype according to TILs level based on transcriptomic data derived from tumor cells. (F) Proportion of immune cells by deconvolutional analysis based on transcriptomic data derived from immune cells.

3.2. Incorporation of PD-L1 to TILs level

PD-L1 is a representative marker associated with T-cell exhaustion and has recently been reported as a prognostic factor in TNBC[26,27]. Thus, we analyzed the clinical significance of PD-L1 in 104 patients with available PD-L1 expression. PD-L1 positivity was defined as the following three criteria: SP142 ≥ 1%, 22C3 CPS ≥ 1, and 22C3 CPS ≥ 10, with positivity rates of 24%, 69%, and 37%, respectively (Figure 4A). When evaluating prognosis based on PD-L1, regardless of the definition used, the PD-L1+ group consistently demonstrated better outcomes than the PD-L1- group (Figure 4B).

The rate of PD-L1 positivity assessed by the SP142 assay was relatively low compared to that assessed by the 22C3 assay, indicating that PD-L1 positivity is defined more broadly by 22C3 (Figure 4C). We also evaluated the relationship between TILs and PD-L1 expression, noting that this relationship varied depending on the antibody used and the cut-off value applied. Approximately half of the patients with high TILs were classified as PD-L1+ when assessed using SP142. In contrast, when defining PD-L1 positivity as 22C3 CPS ≥ 1, most patients with high TILs were PD-L1+. Furthermore, when using 22C3 CPS ≥ 10 as the cutoff for PD-L1 positivity, about 70% of patients with high TILs were classified as PD-L1+ (Figure 4D). Given that TILs and PD-L1 statuses did not always coincide, we analyzed whether combining TIL and PD-L1 could provide a better prognostic assessment.

When we classified the patient cohort into four groups based TILs level and PD-L1 status (TIL+PD-L1+, TIL+PD-L1-, TIL-PD-L1+, and TIL-PD-L1-), PD-L1 positivity was defined as 22C3 CPS ≥ 10 (Figure 5A). This is because of the following reasons: i) 22C3 is used in clinical practice for applying the pembrolizumab in TNBC, and ii) defining PD-L1 positivity as 22C3 CPS ≥ 1 would result in a tiny number of TIL+PD-L1- subtypes, which would affect the distribution of the four subtypes. Among the 104 patients, 26% were TIL+PD-L1+, 11% were TIL+PD-L1-, 11% were TIL-PD-L1+, and 52% were TIL-PD-L1- (Figure 5A). Baseline characteristics were similar across four subtypes (Table 2). Meanwhile, TILs level was highest in the TIL+PD-L1+ group, followed by TIL+PD-L1-, TIL-PD-L1+, and TIL-PD-L1- groups (Figure 5B). Furthermore, the TIL+PD-L1+ group had the most favorable prognosis compared to other subtypes (Figure 5C-D).

Table 2. Baseline characteristics according to TIL-PD-L1 based subtypes.

Variables	TIL+PD-L1+	TIL+PD-L1-	TIL-PD-L1+	TIL-PD-L1-	P-value
Age					0.285
< 50	14 (51.9)	6 (54.5)	8 (66.7)	21 (38.9)	
≥ 50	13 (48.1)	5 (45.5)	4 (33.3)	33 (61.1)	
Tumor grade*					0.132†
1 or 2	4 (15.4)	3 (27.3)	0	15 (27.8)	

3	22 (84.6)	8 (72.7)	12 (100)	39 (72.2)	
Ki-67					0.261†
< 20%	1 (3.7)	1 (9.1)	1 (8.3)	10 (18.6)	
≥ 20%	26 (96.3)	10 (90.9)	11 (91.7)	44 (81.5)	
pT stage					0.780
1	14 (51.9)	6 (54.5)	7 (58.3)	24 (44.4)	
≥ 2	13 (48.1)	5 (45.5)	5 (41.7)	30 (55.6)	
pN status					0.918†
Negative	20 (74.1)	7 (63.6)	9 (75.0)	40 (74.1)	
Positive	7 (25.9)	4 (36.4)	3 (25.0)	14 (25.9)	
Chemotherapy					0.953†
Yes	2 (7.4)	1 (9.1)	1(8.3)	6 (11.1)	
No	25 (92.6)	10 (90.0)	11 (91.7)	48 (88.9)	
Radiotherapy					0.471†
Yes	9 (33.3)	2 (18.2)	6 (50.0)	18 (33.3)	
No	18 (66.7)	9 (81.8)	6 (50.0)	36 (66.7)	

*Missing values.
†*P*-value was obtained from the Fisher's exact test.

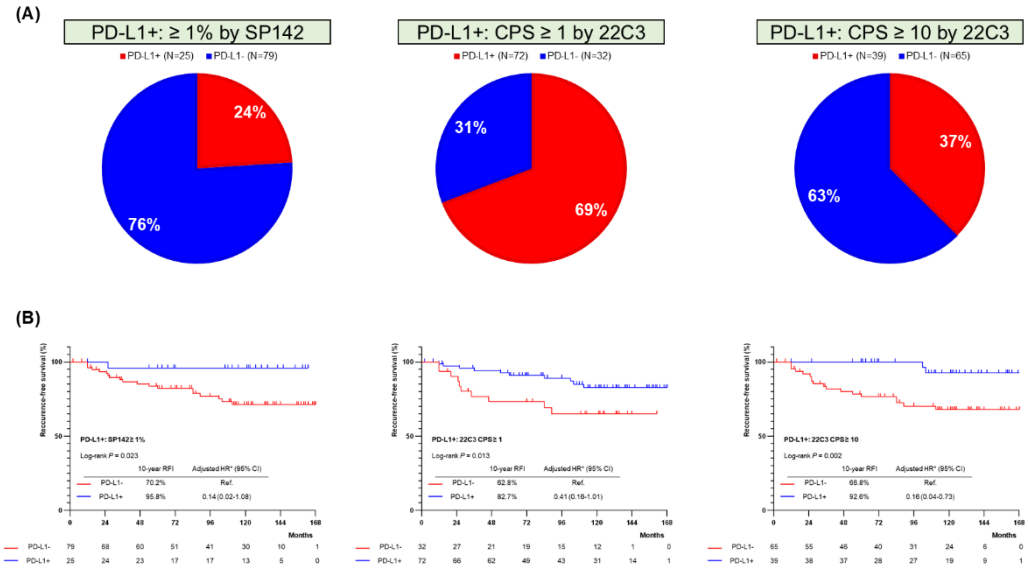

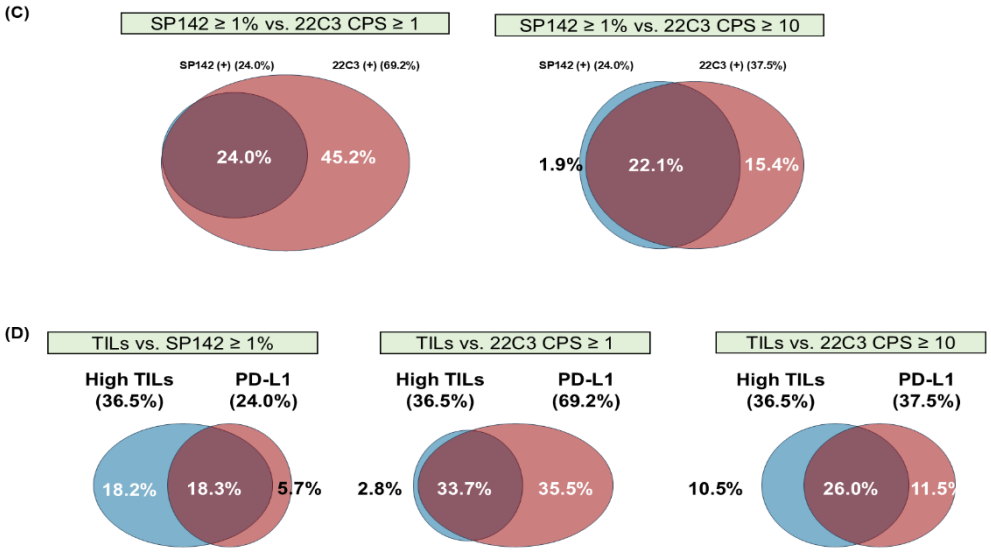

Figure 4. Characteristics by PD-L1 expression. (A) Proportion of PD-L1+ across the PD-L1 antibody assays. (B) Recurrence-free interval according to PD-L1 expression across the PD-L1 antibody assays. (C) Correlation of PD-L1+ between the PD-L1 antibody assays. (D) Correlation between high TILs level and PD-L1 expression across the PD-L1 antibody assays.

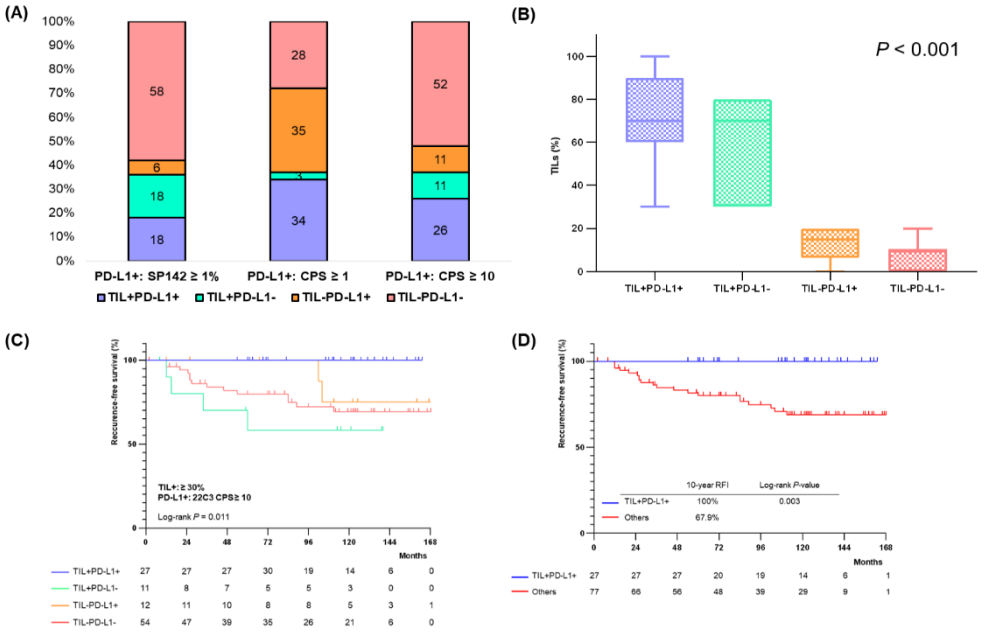

Figure 5. Clinical features by TIL-PD-L1 based subtype. (A) Proportion of TIL-PD-L1 based subtypes. (B) TILs level according to the TIL-PD-L1 based subtypes. (C) Recurrence-free interval (RFI) according to the TIL-PD-L1 based subtypes. (D) Comparison of RFI between TIL+PD-L1+ subtype and others.

3.3. Differences in transcriptomes by TIL-PD-L1 based subtypes

Since the TIL+PD-L1+ subtype demonstrated the most favorable prognosis, we analyzed its distinguishing features compared to other groups. As anticipated, this subtype showed high expression of immune activation-related genes and pathways (e.g., IFN-alpha response, IFN-gamma response, allograft rejection), while immune suppression-related pathways (e.g., EMT signaling, TGF-beta signaling) were expressed at lower levels across the three cell types (Figure 6A-B). Interestingly, similar to the DEG results based on TILs, the number of significant DEGs was low in immune cells (11 genes) compared to tumor cells (122 genes) and stromal cells (90 genes) (Figure 6A). Moreover, the TIL+PD-L1+ subtype had the highest frequency of the BLIA subtype (Figure 6C). We developed a signatures of TIL-PD-L1 based subtypes using the top 163 most differentially expressed genes in tumor cells, and TIL+PD-L1+ signature was associated with a better prognosis in the METABRIC-TNBC dataset (Figure 6D-E).

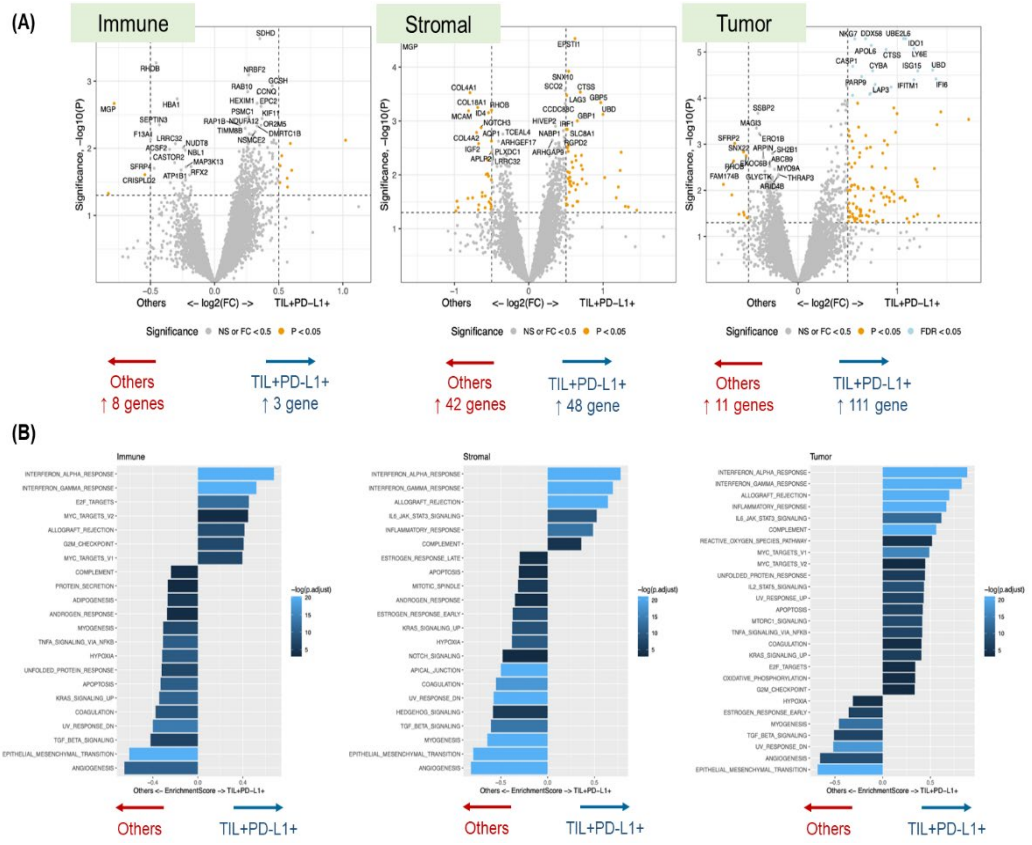

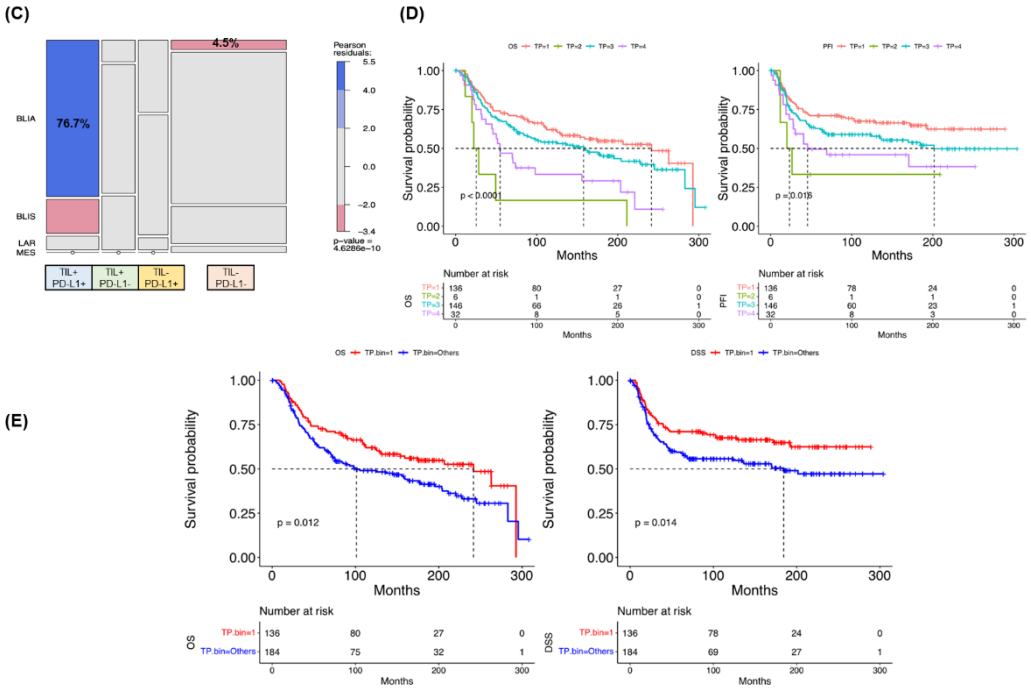

Figure 6. Transcriptomic features of TIL+PD-L1+ subtype. (A) Differentially expressed genes between the TIL+PD-L1+ and other groups. (B) Pathway analyses between the TIL+PD-L1+ and other groups. (C) Proportion of Burstein subtype by TIL-PD-L1 based subtypes derived from the transcriptomic data in tumor cells. (D) Survival outcomes according to the TIL-PD-L1 based subtypes. (D) Comparison of prognosis between TIL+PD-L1+ subtype and others.

By contrast, the TIL-PD-L- subtype was closest to an “immune-cold” tumor in comparison with other subtypes. There were also fewer significant DEGs in immune cells (6 genes) compared to tumor cells (101 genes) and stromal cells (61 genes) (Figure 7A). Pathway analysis revealed a generally higher expression of immune suppression-related pathways in the TIL-PD-L1- subtype, with EMT signaling particularly elevated across all cell types (Figure 7B). Notably, genes with significantly higher expression in the TIL-PD-L1- subtype were predominantly related to stromal fibrosis, particularly in tumor and stromal cells (Figure 7C).

Given the stark differences in prognosis based on PD-L1 expression even among TIL+ cases, we analyzed the differences between TIL+PD-L1+ and TIL+PD-L1- subtypes. DEG results showed that the number of significantly differentially expressed genes was highest in immune cells (96 genes) compared to tumor (65 genes) or stromal cells (79 genes), which is likely due to the presence of immune cells at a certain level in the high TIL group regardless of PD-L1 status (Figure 7D). DEG and pathway analyses generally indicated an immune-activation phenotype in the TIL+PD-L1+ subtype. However, the adipogenesis pathway was uniquely found to have higher expression in the TIL+PD-L1- subtype (Figure 7E). Deconvolution analysis of transcriptomic data derived from immune cells using CIBERSORTx revealed that, compared to TIL+PD-L1+, TIL+PD-L1- had a lower proportion of T-cells and a higher proportion of myeloid cells. Surprisingly, the TIL+PD-L1- subtype also exhibited a higher proportion of B-cells (Figure 7F).

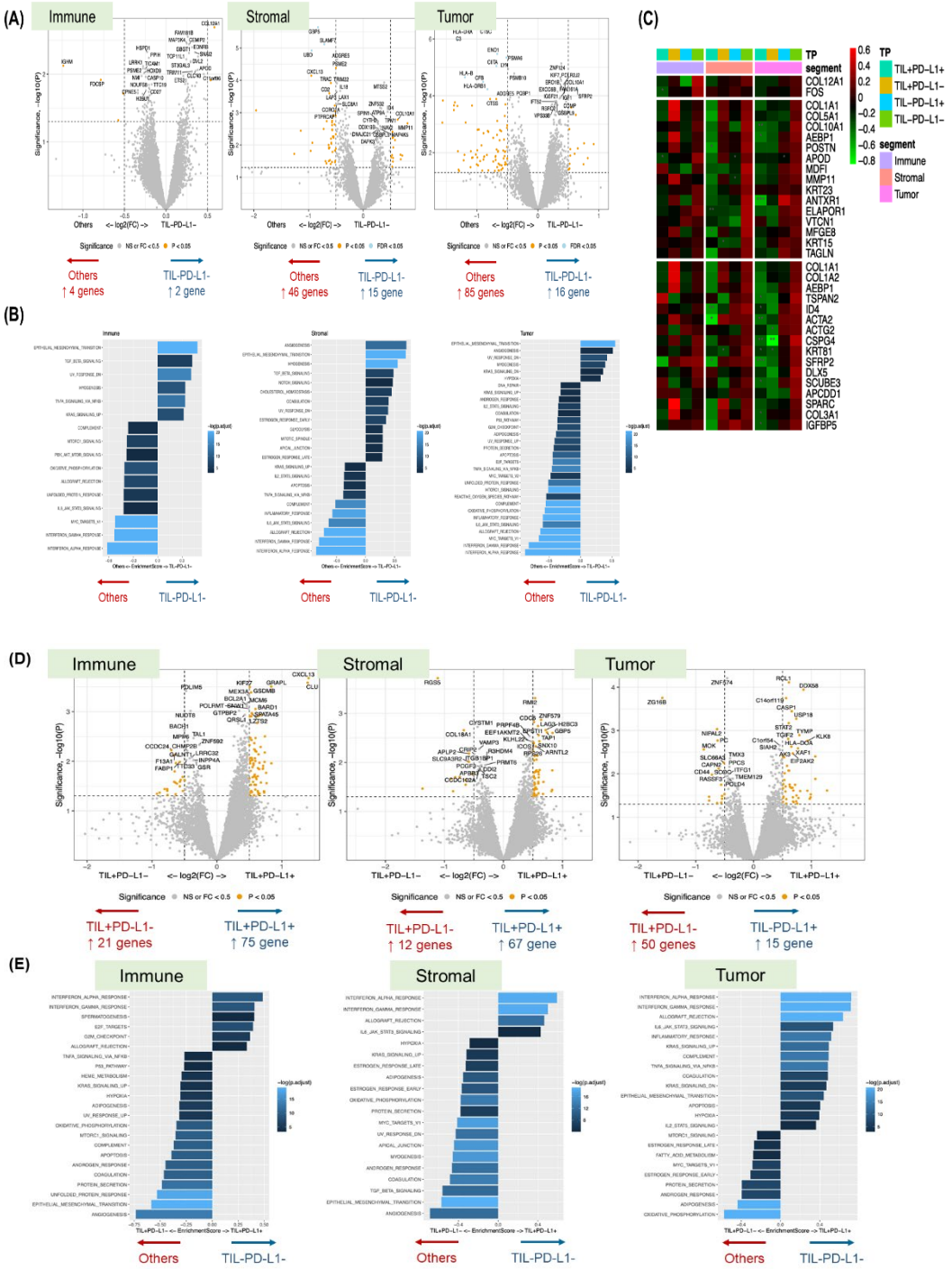

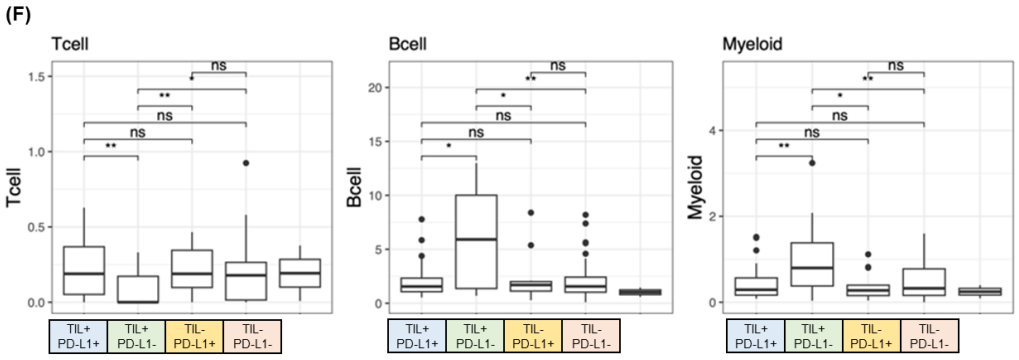

Figure 7. Transcriptomic features of TIL-PD-L1- and TIL+PD-L1- subtypes. (A) Differentially expressed genes between the TIL-PD-L1- and other groups. (B) Pathway analyses between the TIL-PD-L1- and other groups. (C) Expression of genes related to desmoplastic change across the TIL-PD-L1 based subtypes. (D) Differentially expressed genes between the TIL+PD-L1- and TIL+PD-L1+ subtypes. (E) Pathway analyses between the TIL+PD-L1- and TIL+PD-L1+ subtypes. (F) Proportion of immune cells by deconvolutional analysis based on transcriptomic data derived from immune cells across the TIL-PD-L1 based subtypes.

3.4. Characteristics of TIME subtype

Next, we assessed the clinical implications of the TIME subtypes. Of 104 patients, 27% were FI, 20% were SR, 42% were MR, and 11% were ID subtypes (Figure 8A). There were no significant differences in baseline characteristics among the TIME subtypes except tumor grade (Table 3): the proportion of high tumor grade was lowest in the ID subtype (P = 0.011). In contrast, TILs level was highest in the FI, followed by SR, MR, and ID subtypes (Figure 8B-C). Similarly, regardless of the definition method used, the proportion of PD-L1+ was highest in the FI subtype and decreased in the order of SR, MR, and ID (Figure 8D).

When examining the relationship between TIME subtypes and TIL-PD-L1-based subtypes, the TIL+PD-L1+ proportion was highest in the FI subtype, while the TIL-PD-L1- proportion increased progressively from SR to MR to ID (Figure 8E).

Table 3. Baseline characteristics according to TIME subtypes.

Variables	Fully-inflamed	Stromal-restricted	Marginal-restricted	Immune-dessert	*P*-value
Age					0.067
< 50	14 (51.9)	15 (68.2)	17 (38.6)	3 (27.3)	
≥ 50	13 (48.1)	7 (31.8)	27 (61.4)	9 (72.7)	
Tumor grade*					0.017†
1 or 2	3 (11.5)	2 (9.1)	11 (25.0)	6 (54.5)	

3	23 (88.5)	20 (90.9)	33 (75.0)	5 (45.5)	
Ki-67					0.067†
< 20%	0	4 (18.2)	7 (15.9)	2 (18.2)	
≥ 20%	27 (100)	18 (81.8)	37 (84.1)	9 (81.8)	
pT stage					0.993
1	13 (48.1)	11 (50.0)	22 (50.0)	5 (45.5)	
≥ 2	14 (51.9)	11 (50.0)	22 (50.0)	6 (54.5)	
pN status					0.221
Negative	20 (74.1)	13 (59.1)	36 (81.8)	7 (63.6)	
Positive	7 (25.9)	9 (40.9)	8 (18.2)	4 (36.4)	
Chemotherapy					0.574†
Yes	3 (11.1)	1 (4.5)	4 (9.1)	2 (18.2)	
No	24 (88.9)	21 (95.5)	40 (90.9)	9 (81.8)	
Radiotherapy					0.683
Yes	10 (37.0)	5 (22.7)	16 (36.4)	4 (36.4)	
No	17 (63.0)	17 (77.3)	28 (63.6)	7 (63.6)	

*Missing values.
†*P*-value was obtained from the Fisher's exact test.

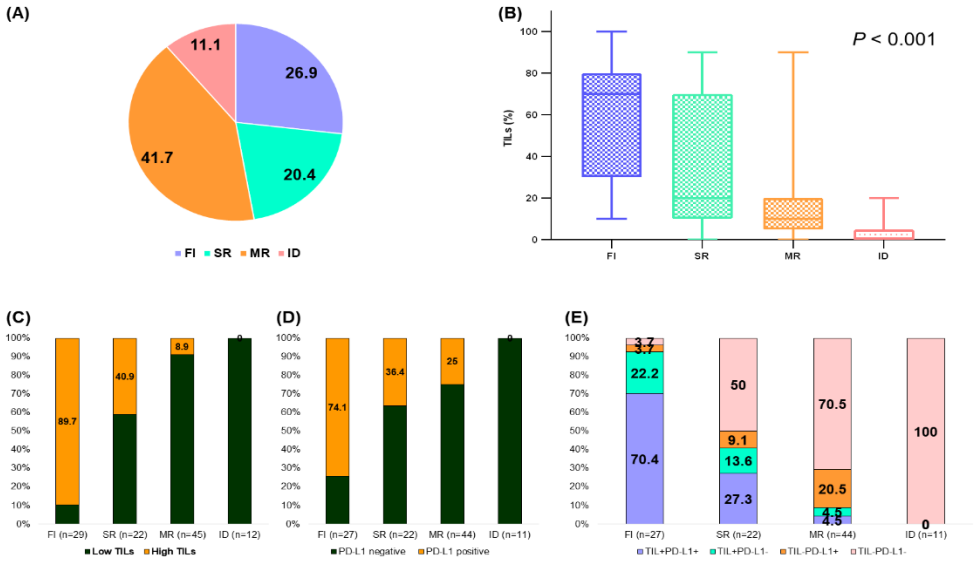

Figure 8. Clinical features by TIME subtype. (A) Proportion of TIME subtype. (B) TILs level according to the TIME subtypes. (C) Proportion of case with TIL+ according to the TIME subtype.

(D) Proportion of case with PD-L1+ according to the TIME subtype. (E) Proportion of TIL-PD-L1 based subtype within the TIME subtype.

3.5. Differences in transcriptomes by TIME subtypes

Considering the TIME subtypes are classified based on the extent of immune cell infiltration, we anticipated that analyzing the mechanisms related to immune cell infiltration would be insightful. Typically, TIME subtypes such as FI and SR are categorized as high TILs, while MR and ID are categorized as low TILs (Figure 8C). Given that the characteristics of MR and ID would be similar to those of the low TIL group, we focused on the comparison between FI and SR to compare FI and SR to understand the mechanisms of immune cell infiltration into the intra-tumoral region.

When comparing FI and SR, a notable observation was that, despite being high TIL groups, the number of DEGs in immune cells (6 genes) was lower compared to tumor (97 genes) or stromal cells (39 genes) (Figure 9A). In DEG analyses, antigen-presenting related genes (e.g. *ICAM1*, *TAP1*, *CD4*, and *HLA-DRA*, etc.) and neoantigen-related oncogenic genes (e.g. *S100A9*, *S100A8*, *LYZ*, *CD74* and *STAT1*, etc.) were expressed at higher levels in tumor cells in the FI subtype than SR[28-30]. Overall, immune activation-related pathways were more highly expressed in FI, and uniquely, apical surface and apical function pathways exhibited higher expression in tumor cells of the FI subtype compared to SR (Figure 9B). In addition, the BLIA subtype was the most prevalent in the FI subtype, closely resembling an ‘immune-hot” tumor (Figure 9C).

3.6. Comparison between TIL+PD-L1+ and TIL+PD-L1- in FI subtype

Finally, we evaluated the differences between TIL+PD-L1+ and TIL+PD-L1- within the FI subtype, where immune cells have infiltrated the intra-tumoral region. In the FI subtype, 70.4% of patients were classified as TIL+PD-L1+ and 22.2% as TIL+PD-L1- (Figure 8E). A striking difference in prognosis was observed between these groups: no recurrences were noted in the TIL+PD-L1+ group, while the 10-year RFI for the TIL+PD-L1- subtype was 60% (Figure 9D).

We compared the expression of immune cell activation-related genes within immune cells across tumor, immune, and stromal cell types (Figure 9E). Immune cell activation-related genes exhibited higher expression levels in the TIL+PD-L1+ subtype compared to the TIL+PD-L1- subtype. Notably, genes related to resident CD4 T cell activation (SELL, TCF7), CD4 T cell activation (IL4R), and CD8 T cell cytotoxicity (GZMK, PRF1) were significantly expressed in the TIL+PD-L1+ subtype compared to the TIL+PD-L1- subtype (Figure 9E).

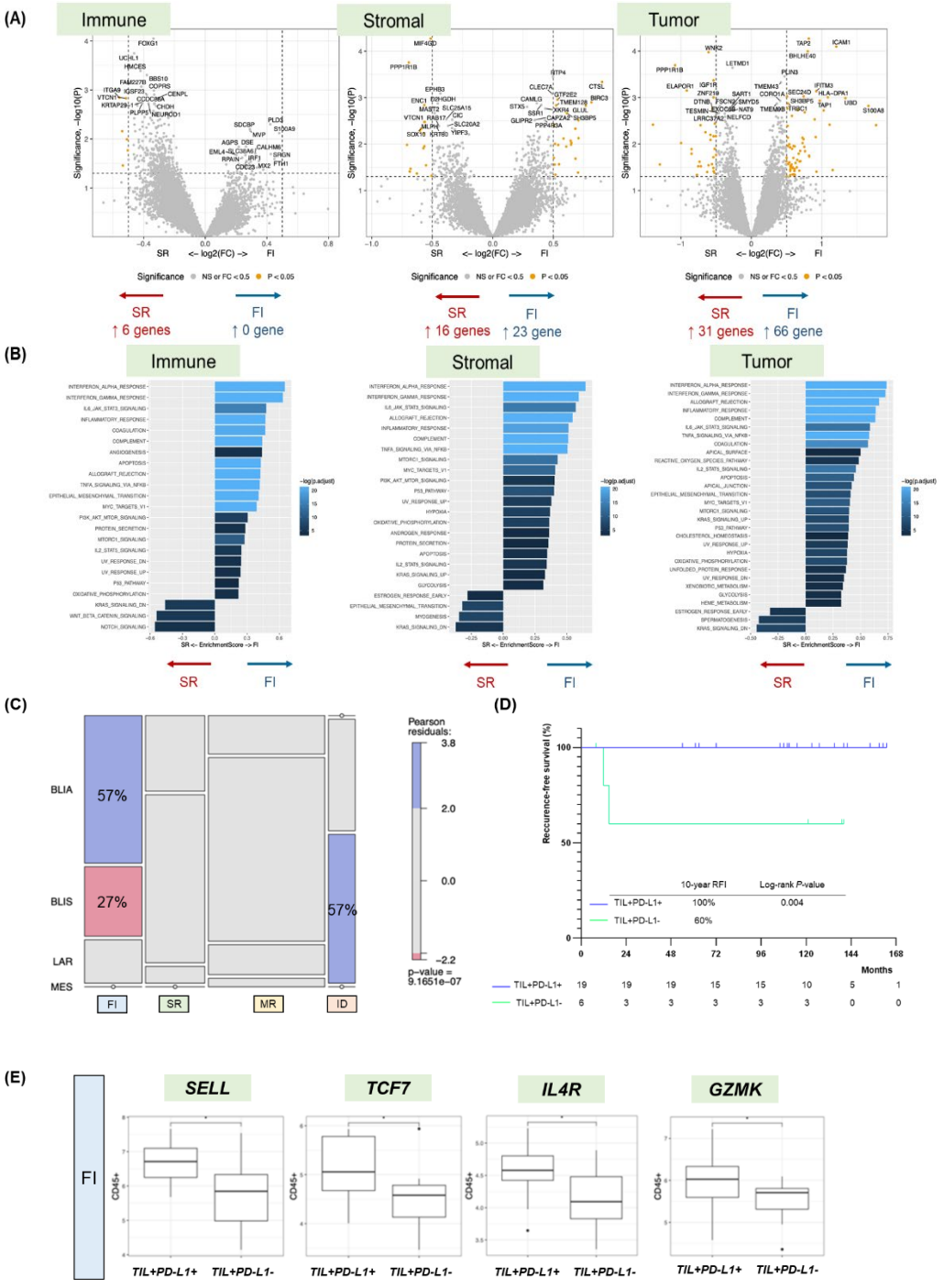

Figure 9. Transcriptomic features by TIME subtype. (A) Differentially expressed genes between the FI and SR subtypes. (B) Pathway analyses between the FI and SR subtypes. Clinical features by tumor-immune microenvironment (TIME) subtype. (C) Proportion of Burstein subtype TIME subtypes derived from the transcriptomic data in tumor cells. (D) Comparison of recurrence-free-interval between TIL+PD-L1+ and TIL+PD-L1- subtypes within the FI subtype. (E) Expression of immune system activation-related genes in the immune cells between TIL+PD-L1+ and TIL+PD-L1- subtypes within the FI subtype.

IV. DISCUSSION

Herein, we analyzed the landscape of TNBC not only in terms of TILs level but also based on PD-L1 expression and TIME subtypes. This approach was taken because we believe that, in addition to the quantity of immune cells within or near the tumor tissue (as represented by TILs level), the activity of these immune cells (as represented by PD-L1 expression) and the degree of immune cell infiltration (the distance between immune cells and tumor cells, as represented by TIME subtype) are also crucial. We identified that TILs level, as well as PD-L1 expression, serves as an independent prognostic factor. Interestingly, when TIL levels and PD-L1 expression were combined, a more distinct stratification was observed, highlighting the potential clinical application of TILs and PD-L1 as combined biomarkers in triple-negative breast cancer. Furthermore, consistent with the findings of previous studies, we also found that the majority of high TILs are classified into the FI and SR among the TIME subtypes, while most low TILs fall into the MR and ID subtypes[23].

Immune-activated phenotypes (characterized by high TIL, TIL+PD-L1+, or FI groups) exhibited upregulation of immune system activation pathways, including IFN-alpha and -gamma responses, allograft rejection, and inflammatory responses. Conversely, immune-suppressed phenotypes showed activation of pathways commonly associated with tumor progression, such as EMT, angiogenesis, TGF-beta signaling, and estrogen response. The latter is notably linked to the luminal androgen receptor (LAR) subtype of TNBC, which usually displays an immune-suppressed phenotype[16,25].

The strength of this study lies in its ability to compare differences between immune-activated and immune-suppressed phenotypes across tumor, immune, and stromal cell types using spatial transcriptomic profiler. Interestingly, our transcriptomic analysis based solely on tumor cells revealed a higher proportion of the BLIA subtype in immune-activated groups[25]. Furthermore, the number of DEGs between immune phenotypes was significantly greater in tumor cells than in immune cells, suggesting that tumor factors may play a more pivotal role in determining the immune phenotype than host factors[31]. However, this observation could partly be due to the relatively lower abundance of immune cells in the immune-suppressive groups (such as the low TILs group and the MR & ID TIME subtypes). Additionally, since RNA-sequencing was performed on pooled CD45+ immune cells, it might have obscured specific characteristics of individual immune cell types. Single-cell RNA-sequencing based analysis, which captures the diversity of immune cell populations, may provide deeper insights into the phenotypic variations within immune cells regarding immune system regulation in TNBC[32,33].

Among the TIL-PD-L1-based subtypes, TIL+PD-L1+ demonstrated the most favorable prognosis, characterizing it as a "hot" tumor. Furthermore, the TIL+PD-L1+ signature, developed based on DEGs in tumor cells, was validated as a prognostic tool using public gene datasets. Recent research suggests that having a favorable immune phenotype in TNBC may allow for treatment de-escalation. The NeoPACT trial, which omitted the anthracycline chemotherapy from the

KEYNOTE-522 regimen, showed that an activated immune phenotype—characterized by high TILs, PD-L1 positivity (CPS ≥ 10 via 22C3 assay), a DNA damage immune response signature, and a TIME signature—was associated with a high pCR rate exceeding 70%[34]. Additionally, for stage I TNBC with high TILs, the omission of adjuvant chemotherapy has been suggested due to low recurrence rates, indicating the potential for chemotherapy de-escalation[35,36]. Thus, it is plausible that treatment de-escalation could be a reliable option for the TIL+PD-L1+ subtype in the future.

In contrast, the TIL-PD-L1- subtype exhibited characteristics of an "immune-cold" tumor: it had the lowest TILs level and predominantly fell into the MR or ID subtypes. In the TIL-PD-L1- subtype, the expression of genes related to tumor fibrosis was elevated, especially in tumor and stromal cells. Notably, the expression of the *SFRP2* gene was particularly high in tumor cells of the TIL-PD-L1- subtype. *SFRP2* has been reported to promote angiogenesis through Wnt-signaling activation, leading to tumor progression and poor prognosis in breast cancer[37-40.] Additionally, in other cancer types, *SFRP2* has been associated with fibroblast activation and stromal fibrosis, facilitating EMT and immune evasion[41-43]. These findings support the notion that the TIL-PD-L1- subtype induces desmoplastic changes, thereby suppressing immune cell infiltration[44-46]. This subtype is anticipated to have the poorest response with immunotherapy, representing approximately 50% of the TNBC population, underscoring the need for novel therapeutic strategies. Further research focusing on genes with markedly increased expression in the TIL-PD-L1- subtype, such as *SFRP2*, as potential therapeutic targets is warranted.

Because the TIL+PD-L1- subtype had a high TILs level and the absence of PD-L1 associated with T-cell exhaustion, we expected that this subtype had a highly activated immune environment and better clinical outcomes. However, it is intriguingly not characterized as a typical "immune-hot" tumor and exhibits a poorer prognosis compared to TIL+PD-L1+ subtype. Similar findings were observed in the Fudan University multiomics and the Future-C cohorts, where TIL+PD-L1- was associated with an exhausted tumor microenvironment characterized by high infiltration of immunosuppressive immune cells[17]. Our study also showed that this subtype has a low proportion and activity of T cells but a high proportion of myeloid cells. The adipogenesis pathway was uniquely elevated in the TIL+PD-L1- subtype across tumor, stromal, and immune cell types, suggesting the importance of genes associated with this pathway. Notably, the *ZG16B* gene was highly expressed in tumor cells of the TIL+PD-L1- subtype; *ZG16B* has been reported to promote tumor progression by inhibiting T cells through the activation of myeloid-derived suppressor cells in pancreatic cancer[47,48]. Therefore, this gene may represent potential target in future treatment strategies.

When focusing on the TIME subtypes, the majority of ID and MR subtypes corresponded to low TILs, displaying similar transcriptomic features. Consequently, we focused on comparative analysis between the SR and FI subtypes, which fall under the high TIL category, to uncover factors facilitating immune cell infiltration into the intra-tumoral region rather than remaining confined to the stromal region. Consistent with our previous results, the number of DEGs was highest in tumor cells (97 genes), compared to stromal cells (39 genes) and immune cells (6 genes). In the FI subtype, oncogenic processes- or antigen presentation-related genes were upregulated. Furthermore, pathways associated with epithelial cell polarity, such as apical surface and apical junction pathways, were activated in the FI subtype. Accordingly, these factors may induce the immune cell infiltration into the intra-tumoral region.

While most FI subtypes were TIL+PD-L1+, approximately 20% were TIL+PD-L1-. Notably. these two groups showed markedly different prognoses. The TIL+PD-L1- group showed lower expression of genes linked to immune system activation. These results indicate that even with

intratumoral immune cell infiltration, poor prognosis is associated with low immune cell activation, further underscoring the potential role of PD-L1 as a critical biomarker.

Collectively, cases with low TILs, TIL-PD-L1-, and ID/MR TIME subtypes largely overlap, representing "immune-cold" tumors characterized by desmoplastic changes in the surrounding stroma, with genes like *SFRP2* potentially serving as key biomarkers. In comparing SR and FI subtypes, tumor epithelial polarity and antigen presentation appear instrumental in enabling immune cell infiltration into the tumor region. Even in the case of high TILs, there was a significant difference in prognosis as well as immune system activation depending on PD-L1 expression. When limited to the FI subtype, immune activation differed based on PD-L1 expression status, with tumor adipogenesis potentially playing a role in immune cell inactivation, highlighting *ZG16B* as a key gene of interest (Figure 10).

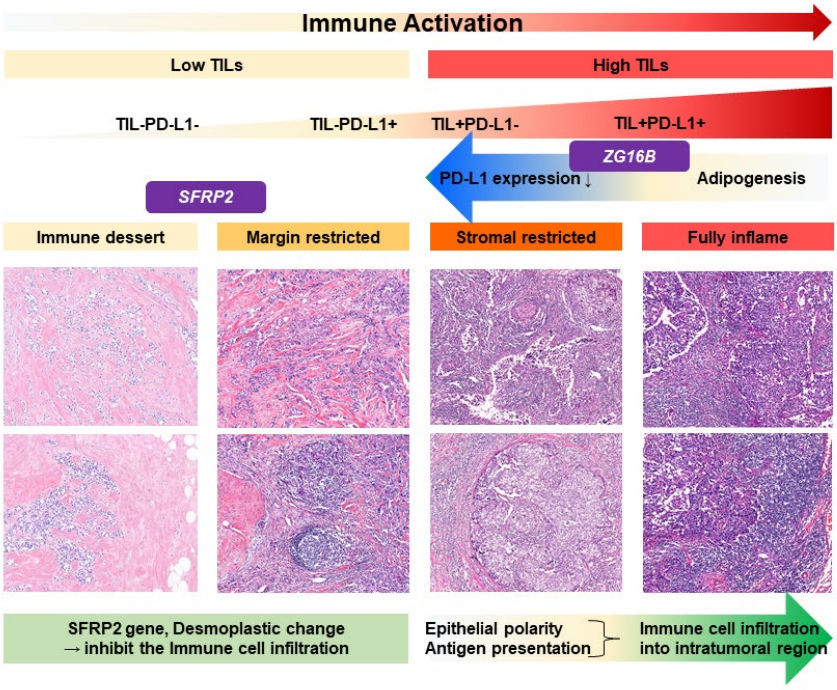

Figure 10. Schematic Overview.

Our study has several limitations. First of all, although we proposed considerable mechanisms and target genes related to the regulation of the immune system in TNBC using a spatial transcriptomic platform, a clear limitation of our research is the lack of further validation of these findings through experimental strategies. Second, this was a retrospective study conducted at a single institution. In particular, the number of patients in each group was relatively small when classified based on the TIL-PD-L1 subtype or TIME subtype into four groups. Third, this study included patients with TNBC who underwent upfront surgery, leading to a substantially high proportion of early-stage patients, such as those in Stage I-II. Recently, patients with stage II-III TNBC have been receiving neoadjuvant chemotherapy plus pembrolizumab. Therefore, it is

necessary to validate the clinical significance of the TIL-PD-L1-based / TIME subtypes or the several target genes in the neoadjuvant setting.

V. CONCLUSION

The primary strength of this study lies in its comprehensive analysis of the immune-related tumor microenvironment, achieved by differentiating between tumor, stromal, and immune cells through digital spatial transcriptomics in a relatively large cohort of patients with TNBC. Our findings underscore the potential clinical utility of TILs and PD-L1 as integrated biomarkers for predicting clinical outcomes and guiding systemic treatment strategies in early-stage TNBC. Moreover, we identified potential key mechanisms and biomarkers associated with variations in immune-related microenvironments. Further experimental validation of these mechanisms and target factors will be crucial in advancing precision medicine for TNBC patients.

References

1. Dent R, Trudeau M, Pritchard KI, Hanna WM, Kahn HK, Sawka CA, et al. Triple-negative breast cancer: clinical features and patterns of recurrence. Clin Cancer Res 2007;13:4429-34.
2. Foulkes WD, Smith IE, Reis-Filho JS. Triple-negative breast cancer. N Engl J Med 2010;363:1938-48.
3. Bianchini G, Balko JM, Mayer IA, Sanders ME, Gianni L. Triple-negative breast cancer: challenges and opportunities of a heterogeneous disease. Nat Rev Clin Oncol 2016;13:674-90.
4. Denkert C, von Minckwitz G, Darb-Esfahani S, Lederer B, Heppner BI, Weber KE, et al. Tumour-infiltrating lymphocytes and prognosis in different subtypes of breast cancer: a pooled analysis of 3771 patients treated with neoadjuvant therapy. Lancet Oncol 2018;19:40-50.
5. Park JH, Jonas SF, Bataillon G, Criscitiello C, Salgado R, Loi S, et al. Prognostic value of tumor-infiltrating lymphocytes in patients with early-stage triple-negative breast cancers (TNBC) who did not receive adjuvant chemotherapy. Ann Oncol 2019;30:1941-9.
6. de Jong VMT, Wang Y, Ter Hoeve ND, Opdam M, Stathonikos N, Jóźwiak K, et al. Prognostic Value of Stromal Tumor-Infiltrating Lymphocytes in Young, Node-Negative, Triple-Negative Breast Cancer Patients Who Did Not Receive (neo)Adjuvant Systemic Therapy. J Clin Oncol 2022;40:2361-74.
7. Schmid P, Adams S, Rugo HS, Schneeweiss A, Barrios CH, Iwata H, et al. Atezolizumab and Nab-Paclitaxel in Advanced Triple-Negative Breast Cancer. N Engl J Med 2018;379:2108-21.
8. Emens LA, Adams S, Barrios CH, Diéras V, Iwata H, Loi S, et al. First-line atezolizumab plus nab-paclitaxel for unresectable, locally advanced, or metastatic triple-negative breast cancer: IMpassion130 final overall survival analysis. Ann Oncol 2021;32:983-93.
9. Cortes J, Rugo HS, Cescon DW, Im SA, Yusof MM, Gallardo C, et al. Pembrolizumab plus Chemotherapy in Advanced Triple-Negative Breast Cancer. N Engl J Med 2022;387:217-26.
10. Cortes J, Cescon DW, Rugo HS, Nowecki Z, Im SA, Yusof MM, et al. Pembrolizumab plus chemotherapy versus placebo plus chemotherapy for previously untreated locally recurrent inoperable or metastatic triple-negative breast cancer (KEYNOTE-355): a randomised, placebo-controlled, double-blind, phase 3 clinical trial. Lancet 2020;396:1817-28.
11. Schmid P, Cortes J, Pusztai L, McArthur H, Kümmel S, Bergh J, et al. Pembrolizumab for Early Triple-Negative Breast Cancer. N Engl J Med 2020;382:810-21.
12. Schmid P, Cortes J, Dent R, Pusztai L, McArthur H, Kümmel S, et al. Event-free Survival with Pembrolizumab in Early Triple-Negative Breast Cancer. N Engl J Med 2022;386:556-67.
13. Pusztai L, Denkert C, O'Shaughnessy J, Cortes J, Dent R, McArthur H, et al. Event-free survival by residual cancer burden with pembrolizumab in early-stage TNBC: exploratory analysis from KEYNOTE-522. Ann Oncol 2024;35:429-36.
14. Haanen J, Obeid M, Spain L, Carbonnel F, Wang Y, Robert C, et al. Management of toxicities from immunotherapy: ESMO Clinical Practice Guideline for diagnosis, treatment and follow-up. Ann Oncol 2022;33:1217-38.

15. Nederlof I, Voorwerk L, Kok M. Facts and Hopes in Immunotherapy for Early-Stage Triple-Negative Breast Cancer. Clin Cancer Res 2023;29:2362-70.
16. Jiang YZ, Ma D, Suo C, Shi J, Xue M, Hu X, et al. Genomic and Transcriptomic Landscape of Triple-Negative Breast Cancers: Subtypes and Treatment Strategies. Cancer Cell 2019;35:428-40.e5.
17. Wang H, Ding XH, Liu CL, Xiao Y, Shui RH, Li YP, et al. Genomic alterations affecting tumor-infiltrating lymphocytes and PD-L1 expression patterns in triple-negative breast cancer. J Natl Cancer Inst 2023;115:1586-96.
18. Salgado R, Denkert C, Demaria S, Sirtaine N, Klauschen F, Pruneri G, et al. The evaluation of tumor-infiltrating lymphocytes (TILs) in breast cancer: recommendations by an International TILs Working Group 2014. Ann Oncol 2015;26:259-71.
19. Cha YJ, Ahn SG, Bae SJ, Yoon CI, Seo J, Jung WH, et al. Comparison of tumor-infiltrating lymphocytes of breast cancer in core needle biopsies and resected specimens: a retrospective analysis. Breast Cancer Res Treat 2018;171:295-302.
20. Loi S, Michiels S, Adams S, Loibl S, Budczies J, Denkert C, et al. The journey of tumor-infiltrating lymphocytes as a biomarker in breast cancer: clinical utility in an era of checkpoint inhibition. Ann Oncol 2021;32:1236-44.
21. Loi S, Drubay D, Adams S, Pruneri G, Francis PA, Lacroix-Triki M, et al. Tumor-Infiltrating Lymphocytes and Prognosis: A Pooled Individual Patient Analysis of Early-Stage Triple-Negative Breast Cancers. J Clin Oncol 2019;37:559-69.
22. Cha YJ, Kim D, Bae SJ, Ahn SG, Jeong J, Lee HS, et al. PD-L1 expression evaluated by 22C3 antibody is a better prognostic marker than SP142/SP263 antibodies in breast cancer patients after resection. Sci Rep 2021;11:19555.
23. Gruosso T, Gigoux M, Manem VSK, Bertos N, Zuo D, Perlitch I, et al. Spatially distinct tumor immune microenvironments stratify triple-negative breast cancers. J Clin Invest 2019;129:1785-800.
24. Tolaney SM, Garrett-Mayer E, White J, Blinder VS, Foster JC, Amiri-Kordestani L, et al. Updated Standardized Definitions for Efficacy End Points (STEEP) in Adjuvant Breast Cancer Clinical Trials: STEEP Version 2.0. J Clin Oncol 2021;39:2720-31.
25. Burstein MD, Tsimelzon A, Poage GM, Covington KR, Contreras A, Fuqua SA, et al. Comprehensive genomic analysis identifies novel subtypes and targets of triple-negative breast cancer. Clin Cancer Res 2015;21:1688-98.
26. Matikas A, Zerdes I, Lövrot J, Richard F, Sotiriou C, Bergh J, et al. Prognostic Implications of PD-L1 Expression in Breast Cancer: Systematic Review and Meta-analysis of Immunohistochemistry and Pooled Analysis of Transcriptomic Data. Clin Cancer Res 2019;25:5717-26.
27. Yeong J, Lim JCT, Lee B, Li H, Ong CCH, Thike AA, et al. Prognostic value of CD8 + PD-1+ immune infiltrates and PDCD1 gene expression in triple negative breast cancer. J Immunother Cancer 2019;7:34.
28. Zhang X, Niu M, Li T, Wu Y, Gao J, Yi M, et al. S100A8/A9 as a risk factor for breast cancer negatively regulated by DACH1. Biomark Res 2023;11:106.
29. Gu Z, Wang L, Dong Q, Xu K, Ye J, Shao X, et al. Aberrant LYZ expression in tumor cells serves as the potential biomarker and target for HCC and promotes tumor progression via csGRP78. Proc Natl Acad Sci U S A 2023;120:e2215744120.
30. Kelly A, Trowsdale J. Genetics of antigen processing and presentation. Immunogenetics 2019;71:161-70.

31. Ogino S, Galon J, Fuchs CS, Dranoff G. Cancer immunology--analysis of host and tumor factors for personalized medicine. Nat Rev Clin Oncol 2011;8:711-9.
32. Chung W, Eum HH, Lee HO, Lee KM, Lee HB, Kim KT, et al. Single-cell RNA-seq enables comprehensive tumour and immune cell profiling in primary breast cancer. Nat Commun 2017;8:15081.
33. Wu SZ, Al-Eryani G, Roden DL, Junankar S, Harvey K, Andersson A, et al. A single-cell and spatially resolved atlas of human breast cancers. Nat Genet 2021;53:1334-47.
34. Sharma P, Stecklein SR, Yoder R, Staley JM, Schwensen K, O'Dea A, et al. Clinical and Biomarker Findings of Neoadjuvant Pembrolizumab and Carboplatin Plus Docetaxel in Triple-Negative Breast Cancer: NeoPACT Phase 2 Clinical Trial. JAMA Oncol 2024;10:227-35.
35. Leon-Ferre RA, Jonas SF, Salgado R, Loi S, de Jong V, Carter JM, et al. Tumor-Infiltrating Lymphocytes in Triple-Negative Breast Cancer. Jama 2024;331:1135-44.
36. Geurts VCM, Balduzzi S, Steenbruggen TG, Linn SC, Siesling S, Badve SS, et al. Tumor-Infiltrating Lymphocytes in Patients With Stage I Triple-Negative Breast Cancer Untreated With Chemotherapy. JAMA Oncol 2024;10:1077-86.
37. van Loon K, Huijbers EJM, Griffioen AW. Secreted frizzled-related protein 2: a key player in noncanonical Wnt signaling and tumor angiogenesis. Cancer Metastasis Rev 2021;40:191-203.
38. Huang C, Ye Z, Wan J, Liang J, Liu M, Xu X, et al. Secreted Frizzled-Related Protein 2 Is Associated with Disease Progression and Poor Prognosis in Breast Cancer. Dis Markers 2019;2019:6149381.
39. Hill VK, Ricketts C, Bieche I, Vacher S, Gentle D, Lewis C, et al. Genome-wide DNA methylation profiling of CpG islands in breast cancer identifies novel genes associated with tumorigenicity. Cancer Res 2011;71:2988-99.
40. Courtwright A, Siamakpour-Reihani S, Arbiser JL, Banet N, Hilliard E, Fried L, et al. Secreted frizzle-related protein 2 stimulates angiogenesis via a calcineurin/NFAT signaling pathway. Cancer Res 2009;69:4621-8.
41. Siegel JB, Nasarre P, Hsu L, Mukherjee R, Gormley M, Richardson B, et al. Secreted frizzled related-protein 2 is prognostic for human pancreatic cancer patient survival and is associated with fibrosis. Cancer Biomark 2023;38:287-300.
42. Vincent KM, Postovit LM. A pan-cancer analysis of secreted Frizzled-related proteins: re-examining their proposed tumour suppressive function. Sci Rep 2017;7:42719.
43. Sun Y, Zhu D, Chen F, Qian M, Wei H, Chen W, et al. SFRP2 augments WNT16B signaling to promote therapeutic resistance in the damaged tumor microenvironment. Oncogene 2016;35:4321-34.
44. Chen S, Wei Y, Liu H, Gong Y, Zhou Y, Yang H, et al. Analysis of Collagen type X alpha 1 (COL10A1) expression and prognostic significance in gastric cancer based on bioinformatics. Bioengineered 2021;12:127-37.
45. Wang Q, Wang K, Tan X, Li Z, Wang H. Immunomodulatory role of metalloproteases in cancers: Current progress and future trends. Front Immunol 2022;13:1064033.
46. Song Y, Wang L, Wang K, Lu Y, Zhou P. COL12A1 Acts as a Novel Prognosis Biomarker and Activates Cancer-Associated Fibroblasts in Pancreatic Cancer through Bioinformatics and Experimental Validation. Cancers (Basel) 2023;15.
47. Song J, Lee J, Kim J, Jo S, Kim YJ, Baek JE, et al. Pancreatic adenocarcinoma up-regulated factor (PAUF) enhances the accumulation and functional activity of myeloid-derived suppressor cells (MDSCs) in pancreatic cancer. Oncotarget 2016;7:51840-53.

48. Lee Y, Kim SJ, Park HD, Park EH, Huang SM, Jeon SB, et al. PAUF functions in the metastasis of human pancreatic cancer cells and upregulates CXCR4 expression. Oncogene 2010;29:56-67.

Abstract in Korean

삼중음성유방암의 면역 조절과 관련된 종양미세환경 규명

삼중음성유방암은 매우 이질적이고 공격적인 아형이지만, 면역 조절과 연관된 종양미세환경의 특징 및 분자생물학적 기전은 여전히 불분명하다. 본 연구는 tumor-infiltrating lymphocytes (TILs), programmed cell death 1 ligand 1 (PD-L1), 종양 내 TILs 의 침윤 정도를 평가하는 tumor-immune microenvironment (TIME) subtype 을 기반으로 삼중음성유방암의 면역관련 종양미세환경을 분석하였다. 또한, GeoMX Digital Spatial Profiler 를 활용하여 공간적으로 종양, 면역, 그리고 기질 세포를 구분한 후 전사체 프로파일링을 수행하여 면역 활성화 및 면역 억제 표현형 간의 비교분석을 수행하였다.

높은 TILs, PD-L1 양성, 그리고 종양 세포와 TIL 간의 거리가 가까운 경우 면역 활성화 표현형을 보였다. 이러한 표현형은 basal-like immune-activated subtype 으로 분류되는 비율이 높았으며, 이미 잘 알려진 면역 관련 경로의 상향 조절도 관찰되었다. 반면, 면역 억제 표현형은 상피-중배엽 전이, TGF-베타 신호, 혈관신생과 같은 종양 진행과 관련된 경로와 연관되어 있었다. 특히, 종양, 면역, 그리고 기질 세포 중에서 면역 관련 표현형에 따라 관찰된 차등 발현 유전자 수가 종양 세포에서 높았었는데, 이는 종양 세포가 면역 표현형을 형성하는 데 면역 혹은 기질 세포보다 더 중요한 역할을 할 수 있음을 시사한다.

TIL 및 PD-L1 상태에 따라 환자를 분류한 결과, TIL+PD-L1+ 아형은 가장 좋은 예후를 보였으며, TIL+PD-L1+ 유전자 시그니처 역시 우수한 생존 결과와 연관되어 있었다. 반대로, TIL-PD-L1- 아형은 종양미세환경의 섬유화 (desmoplastic change)로 인해 "차가운" 종양의 특성을 보였다. 흥미롭게도, TIL+PD-L1- 아형은 높은 TIL 수준에도 불구하고 더 나쁜 예후와 연관되어 있었는데, 이는 T-cell의 낮은 비율과 활성도, 높은 비율의 myeloid cells, 그리고 세 가지 세포 유형 전반에 걸친 adipogenesis 경로의 활성화 때문인 것으로 보인다. 특히, TILs 이 종양 내 영역까지 깊게 침투하더라도 PD-L1-이면, 면역 세포의 활성도가 낮은 것으로 나타났다. 이는 높은 TIL 을 가진 환자에서 PD-L1이 면역 체계 상태를 반영하는 중요한 마커임을 부각시킨다.

결론적으로, 본 연구의 결과는 삼중음성유방에서 TIL 과 PD-L1의 발현을 통합한 바이오마커가 임상적으로 중요할 수 있음을 제시한다. 또한, 종양미세환경에 위치한 여러 세포들 중 종양 세포가 면역 표현형을 결정하는 데 중심적인 역할을 할 것으로 추측된다. 그뿐만 아니라, 삼중음성유방암에서 면역 체계 조절과 관련된 잠재적인 분자생물학적 기전 및 표적 유전자들을 제시하였는데, 이를 기반으로, 삼중음성유방암 환자의 생존율 향상을 위한 표적 치료제의 개발과 관련된 향후 연구가 필요하다.

핵심되는 말 : 삼중음성유방암, 종양침윤림프구, 프로그램 세포 사멸 리간드 1, 종양

면역미세환경, 공간 전사체.